Journal of Magnetic Resonance **141,** 78–90 (1999)
Article ID jmre.1999.1865, available online at http://www.idealibrary.com on IDEAL®

# Magnitudes and Orientations of Interaction Tensors Determined from Rotational Resonance MAS NMR Lineshapes of a Four-$^{13}$C-Spin System

Stephan Dusold,* Heidi Maisel,† and Angelika Sebald*,[1]

*Bayerisches Geoinstitut and †Institut für Anorganische Chemie, Universität Bayreuth, D-95440 Bayreuth, Germany

Received February 19, 1999; revised June 23, 1999

**Possibilities and limitations of iterative lineshape fitting approaches for the complete determination of magnitudes and orientations of NMR interaction tensors in a four-$^{13}$C-spin system from MAS NMR experiments are investigated. The availability of fast and numerically accurate computational methods is an important prerequisite. The model compound chosen for this investigation is the monoammonium salt of maleic acid. Various selectively and fully $^{13}$C-labeled versions of this compound permit a stepwise reduction of the number of unknown parameters, necessary to fully describe the four-$^{13}$C-spin system in the uniformly $^{13}$C-labeled maleate moiety. This stepwise procedure allows one to monitor reliability and accuracy of multiparameter fits of the four-$^{13}$C-spin system itself, as well as to characterize limitations and requirements for such fitting procedures. Satisfactory $^{1}$H-decoupling performance is an essential experimental requirement; TPPM decoupling yields $n = 1, 2$ rotational resonance $^{13}$C MAS NMR lineshapes suitable for analysis by iterative lineshape fitting methods. It is demonstrated that assumptions about "typical" chemical shielding tensor orientations, even if not deviating much from the real orientations, lead to severe errors in internuclear distance determinations.** © 1999 Academic Press

*Key Words:* **solid-state NMR; magic-angle spinning; homonuclear spin systems; spectral lineshape simulations; rotational resonance.**

## INTRODUCTION

Magic-angle spinning (MAS) NMR spectra of the majority of spin-$\frac{1}{2}$ isotopes usually are straightforward to obtain from powder samples of a very wide range of different chemicals. MAS NMR spectra of spatially isolated, single spin-$\frac{1}{2}$ isotopes (such as, e.g., $^{13}$C, $^{15}$N, $^{29}$Si in low natural abundance) provide easy access to high spectral resolution and to magnitudes of chemical shielding tensors, but do not generally reflect the orientation of chemical shielding tensors in the molecular or crystal principal axis system. The situation differs fundamentally for MAS NMR spectra of isolated homonuclear spin systems, composed of mutually dipolar-coupled spin-$\frac{1}{2}$ isotopes, where spectra depend on both magnitudes and orientations of all interaction tensors (chemical shielding, dipolar and *J* coupling) present within the spin system. Numerically exact spectral lineshape-simulation methods in conjunction with iterative fitting procedures are then required to extract the various interaction parameters from suitable experimental MAS NMR spectra. The smallest spin system where geometrical information is encoded in simple MAS NMR spectra is isolated homonuclear pairs of spin-$\frac{1}{2}$ isotopes. These occur quite commonly in a variety of chemicals, either by spatial separation in the solid-state structure for 100% naturally abundant spin-$\frac{1}{2}$ isotopes (e.g., $^{31}$P, even $^{1}$H, $^{19}$F), or manmade by means of selective enrichment of isotopes of low natural abundance (e.g., $^{13}$C, $^{15}$N in organic molecules). It has been demonstrated that indeed the properties of isolated homonuclear spin-$\frac{1}{2}$ pairs can be exploited for the determination of internuclear distances and/or chemical shielding tensor orientations from straightforward MAS NMR spectra (*1–17*). The accuracy of combined MAS NMR/spectral lineshape fitting approaches can be comparable to that achieved in NMR experiments on oriented single crystals (*16*).

Combined MAS NMR/spectral lineshape fitting strategies have their attractions for the obvious reason that polycrystalline powder samples are far more plentiful and much easier to obtain than are single crystals, suitable for NMR experiments. Much progress has been made recently with regard to the efficiency of numerically exact simulations of MAS NMR spectra (*18–23*). State-of-the-art numerical simulation methods permit full calculation of the MAS NMR spectrum of an isolated homonuclear spin-$\frac{1}{2}$ pair within 1–2 s, using standard computing equipment. Such computational efficiencies not only enable one to employ careful iterative fitting procedures for the extraction of all NMR parameters of an isolated homonuclear spin-$\frac{1}{2}$ pair, but also set the scene to possibly consider MAS NMR spectra of larger isolated homonuclear spin systems for full analysis by means of iterative lineshape fitting methods.

The motivation for an extension toward larger spin systems under MAS NMR conditions is twofold. First, with regard to

[1] Current address: Division of Physical Chemistry, Arrhenius Laboratory, Stockholm University, S-10691 Stockholm, Sweden.



1090-7807/99 $30.00

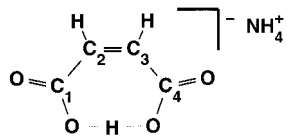

**SCHEME 1.** Schematic illustration of the geometry of the planar maleate moiety; angles and distances are drawn to scale according to the single-crystal X-ray structure (*26*); the numbering scheme C1 to C4 will be maintained throughout the text.

sample properties, (i) it is not normally possible or practical to isotopically deplete 100% naturally abundant isotopes such as $^{31}$P, and not all problems posed to MAS NMR involving $^{31}$P or other 100% naturally abundant spin-$\frac{1}{2}$ isotopes represent isolated spin-pair circumstances, but rather belong to the category of larger isolated, dipolar-coupled homonuclear spin systems; and (ii) even if, e.g., $^{13}$C, $^{15}$N can be pairwise selectively enriched if need arises, occasionally it may turn out to be more economical and desirable to carry out NMR work on multiply or fully labeled samples. Second, beyond such aspects of properties and availability of samples, there is another, basic driving force behind attempts to proceed toward larger dipolar-coupled spin systems. Isolated homonuclear spin pairs in the general case will yield only relative tensor orientations, or otherwise may leave us with a twofold ambiguity concerning assignment. In contrast, isolated spin systems composed of more than two dipolar-coupled spin-$\frac{1}{2}$ isotopes hold the promise of extracting absolute orientational information from simple MAS NMR spectra, as long as we can significantly determine magnitudes and orientations of all interaction tensors from iterative lineshape fitting procedures. We may rephrase this statement in terms of molecular structure as a possibility to unequivocally determine the geometry of a molecular fragment (or even an entire molecule) from straightforward MAS NMR spectra. In the following this option will be explored for a spin system composed of four dipolar-coupled $^{13}$C spins in a molecule of known structure, where, in addition, we have a realistic chance to back up, check, and question every four-spin-system aspect (experimentally, as well as regarding numerical procedures) by additional consideration of selectively labeled two-spin subsets of the spin system. The compound we have chosen for this study is the monoammonium salt of maleic acid (Scheme 1) in various degrees and permutations of $^{13}$C enrichment. These include the compound with $^{13}$C in natural abundance (**1**), a sample where C1 and C4 are selectively $^{13}$C-enriched (**1-C1/C4**), another sample selectively $^{13}$C-enriched at C2 and C3 (**1-C2/C3**), the fully $^{13}$C-enriched version (**1-U$^{13}$C**), and a sample composed of 10 mol% **1-U$^{13}$C** in 90 mol% **1** (**1-U$^{13}$C in 1**).

## EXPERIMENTAL

*Compounds.* All samples of monoammonium salts of maleic acid were obtained from the reaction of commercially available maleic acid anhydrides (natural abundance $^{13}$C content, Aldrich Chemicals; C1/4 $^{13}$C-labeled, C2/3 $^{13}$C-labeled, and fully $^{13}$C-enriched, Promochem, Wesel, Germany) with one equivalent of $(NH_4)(HCO_3)$ in $H_2O$ at ambient conditions in the dark. The monoammonium salts of maleic acid were isolated from the aqueous solutions by slow evaporation of the solvent *in vacuo*. **1-U$^{13}$C in 1** was made by cocrystallization of the two components. All products were obtained in virtually quantitative yield as colorless polycrystalline powders. Identity and purity of all samples were checked by solution-state $^1$H and $^{13}$C NMR.

*NMR experiments.* Solution-state $^1$H ($\omega_0/2\pi = -500.1$ MHz) and $^{13}$C ($\omega_0/2\pi = -125.8$ MHz) NMR spectra (solvent $D_2O$) were recorded on a Bruker DRX 500 NMR spectrometer. $^{13}$C MAS NMR spectra were recorded on Bruker MSL 200, MSL 300, DSX 400, and DSX 500 NMR spectrometers (corresponding to $^{13}$C Larmor frequencies of $-50.3$, $-75.5$, $-100.6$, and $-125.8$ MHz, respectively), using standard double-bearing probes and $ZrO_2$ rotors (4 mm diameter). Spinning frequencies were in the range 0.9–9.0 kHz and were actively controlled to within $\pm 2$ Hz using homebuilt equipment. $^{13}$C MAS NMR spectra of **1-U$^{13}$C** used for the extraction of parameters from iterative lineshape fitting were obtained with single-pulse $^{13}$C excitation (recycle delay 60 min), as well as with Hartmann–Hahn cross polarization (CP, recycle delay 5 s, and a range of CP contact times (1–5 ms)). For the pairwise-labeled compounds **1-C1/C4** and **1-C2/C3,** $^{13}$C CP/MAS NMR spectra served as experimental data for iterative lineshape fitting. $^{13}$C MAS NMR spectra run on the MSL 200 and MSL 300 NMR spectrometers were obtained using on-resonance $^1$H cw decoupling with decoupling field strengths in the range 70–100 kHz. $^{13}$C MAS NMR spectra run on the DSX 400 and DSX 500 NMR spectrometers employed the TPPM decoupling scheme (*24*) and a decoupling field strength of 105 kHz. $^{13}$C chemical shielding is given relative to external $Si(CH_3)_4$, $\omega_{iso}^{CS}$ $^{13}$C $= 0$.

*Definitions and numerical simulations.* Shielding notation (*25*) is used throughout; parameters of all interactions $\lambda$ ($\lambda$ = CS, chemical shielding; $\lambda = D$, direct dipolar coupling, $\lambda$ = J, indirect coupling) are reported according to Haeberlen's convention (*26*), where the isotropic part $\omega_{iso}^{\lambda}$, the anisotropy $\delta^{\lambda}$, and the asymmetry parameter $\eta^{\lambda}$ are related to the principal elements of the interaction tensor $\omega^{\lambda}$ as follows: $\omega_{iso}^{\lambda} = (\omega_{xx}^{\lambda} + \omega_{yy}^{\lambda} + \omega_{zz}^{\lambda})/3$, $\delta^{\lambda} = \omega_{zz}^{\lambda} - \omega_{iso}^{\lambda}$, and $\eta^{\lambda} = (\omega_{yy}^{\lambda} - \omega_{xx}^{\lambda})/\delta^{\lambda}$ with $|\omega_{zz}^{\lambda} - \omega_{iso}^{\lambda}| \geq |\omega_{xx}^{\lambda} - \omega_{iso}^{\lambda}| \geq |\omega_{yy}^{\lambda} - \omega_{iso}^{\lambda}|$. For indirect coupling we have $\omega_{iso}^{J} = \pi J_{iso}$, and for direct dipolar coupling $\eta^{D} = 0$, $\omega_{iso}^{D} = 0$, and $\delta_{ij}^{D} = b_{ij} = -\mu_0 \gamma_i \gamma_j \hbar/(4\pi r_{ij}^3)$, where $\gamma_i$, $\gamma_j$, and $r_{ij}$ denote gyromagnetic ratios and internuclear distances of spins $i$ and $j$, respectively. This may not be the most popular choice of notation as far as chemical shielding tensor eigenvalues are concerned. However, for cases where chemical shielding is not the only interaction tensor to be taken into account, Haeberlen's notation permits full and consistent description of all interaction tensors present, including chemical shielding.

Molecular symmetry in solid **1** (*27*) relates sites C1 with C4, and C2 with C3, by a mirror plane perpendicular to the molecular plane. The corresponding relationships of the Euler angles for the two chemical shielding tensors, related by mirror plane symmetry, are $\alpha_j^{CS} = -\alpha_i^{CS}$, $\beta_j^{CS} = \pi - \beta_i^{CS}$, and $\gamma_j^{CS} = \gamma_i^{CS}$. The same relationship applies for the dipolar coupling tensors $\omega_{ij}^D$ where $i, j = 1, 4$ or $i, j = 2, 3$: $\alpha_{ij}^D = -\alpha_{ji}^D$, $\beta_{ij}^D = \pi - \beta_{ji}^D$, $\gamma_j^D = \gamma_i^D$. The crystal frame was chosen to be coincident with the principal axes system of the dipolar interaction tensors $\Omega_{PC}^{D14} = \Omega_{PC}^{D23} = (0, 0, 0)$.

All simulation and fitting programs utilized the GAMMA programming package (*28*). γ-COMPUTE (*20*) and carousel-averaging COMPUTE methods (*21*) were used for numerical calculation of MAS NMR spectra. Powder averaging involved between 232 and 700 angles $\alpha_{CR}$ and $\beta_{CR}$, selected according to the REPULSION (*22*) or Gaussian spherical quadrature (*23*) schemes. Typical times required for calculation of a single MAS NMR spectrum for a spin pair were between 1 and 5 s, and between 1 and 3 min for four-spin systems, using either Silicon Graphics Origin 200 workstations or PCs running Linux. The Migrad method from the MINUIT optimization package (*29*) was used for error minimization of $e^2 = 1/N \sum_{i=1}^{N} (S_{exp}(\omega_i) - S_{calc}(\omega_i))^2$, where $\max(S_{exp}(\omega_i)) = 1$; the MATLAB (*30*) program was used for calculating contour plots and error scans.

## RESULTS AND DISCUSSION

First, we briefly introduce the basic description of the spin dynamics of the one-, two-, and four-$^{13}$C-spin systems in **1, 1-C1/C4, 1-C2/C3,** and **1-U$^{13}$C** under MAS conditions. Next, we follow a step-by-step procedure to reduce the number of unknown tensor parameters. Once all parameters of the four-$^{13}$C-spin system in **1-U$^{13}$C** are determined from this stepwise procedure (including the use of, e.g., selectively pairwise $^{13}$C-labeled samples), we will discuss the reliability, accuracy, and completeness of information one might expect from iterative lineshape fitting in a situation where **1** and **1-U$^{13}$C** are the only available samples.

### *Numerical Simulations and Iterative Fitting*

The Hamiltonian for a homonuclear *n*-spin composed of spin-$\frac{1}{2}$ isotopes and subjected to MAS may be written as

$$H(t) = \sum_{i=1}^{n} \omega_i^{CS}(t) S_{iz} + \sum_{i=1}^{n} \sum_{j>i}^{n} \omega_{ij}^D(t) \times \left[ S_{iz}S_{jz} - \frac{1}{2}(S_{i+}S_{j-} + S_{i-}S_{j+}) \right] + \sum_{i=1}^{n} \sum_{j>i}^{n} \omega_{ij}^J S_i S_j. \quad [1]$$

Anisotropy of the *J* coupling is neglected in Eq. [1] as well as in our simulations. For homonuclear $^{13}$C spin systems this appears a reasonable approximation, given the far dominating nature of chemical shielding and dipolar coupling interactions in such spin systems. The time dependence of each of the anisotropic interactions may be expressed in terms of a Fourier series

$$\omega^{\lambda}(t) = \sum_{m=-2}^{2} \omega_m^{\lambda} \exp(im\omega_r t), \quad [2]$$

where $\omega_r$ is the spinning frequency in angular units and the coefficients take the form

$$\omega_m^{\lambda} = \omega_{iso}^{\lambda}\delta_{m0} + \delta^{\lambda}\left\{ D_{0,-m}^2(\Omega_{PR}^{\lambda}) - \frac{\eta^{\lambda}}{\sqrt{6}} [D_{-2,-m}^2(\Omega_{PR}^{\lambda}) + D_{2,-m}^2(\Omega_{PR}^{\lambda})] \right\} d_{-m,0}^2(\beta_{RL}). \quad [3]$$

$D_{m,m'}^2(\Omega_{IJ}) = \exp(-i\alpha_{IJ}m) d_{m,m'}^2(\beta_{IJ}) \exp(-i\gamma_{IJ}m')$ is an element of the Wigner rotation matrix describing transformation from an axes system *I* to an axes system *J* related by the Euler angles $\Omega_{IJ} = (\alpha_{IJ}, \beta_{IJ}, \gamma_{IJ})$, where *I* and *J* represent the principal axes system (P) of the interaction, the crystal axes system (C), the rotor axes system (R), or the laboratory axes system (L).

The suitable range of MAS frequencies to determine orientational parameters from MAS NMR spectra depends on the choice of external magnetic field strength and, more importantly, on the differences in isotropic chemical shieldings $\omega_{iso}^{\Delta}$ present in the spin system. When $\omega_{iso}^{\Delta}$ is a small integer multiple of the spinning frequency the so-called rotational resonance condition ($\omega_{iso}^{\Delta} = n\omega_r$, $n = 1, 2, \ldots$) is fulfilled. At these specific MAS frequencies, MAS NMR spectra sensitively reflect magnitudes *and* orientations of the anisotropic interactions (*1–7*). A special case of rotational resonance condition exists for spin pairs with $\omega_{iso}^{\Delta} = 0$: here the so-called $n = 0$ rotational resonance condition is maintained at all spinning frequencies.

An important requirement for the applicability of iterative lineshape fitting methods is the availability of fast computational methods. Speed of computation without sacrificing accuracy becomes increasingly important the larger the spin systems are. Already for our four-$^{13}$C-spin system a relatively large Hilbert-space dimension causes relatively slow numerical matrix manipulation steps, in addition to a large number of fit parameters requiring a large number of iterative steps to reach convergence of the fitting procedure. The COMPUTE approach (*18*), or improved versions thereof (*19–21*), provides a particularly suitable way of performing this simulation task for small- to medium-sized spin systems. Especially those meth-

**TABLE 1**
**$^{13}$C NMR Parameters of 1-U$^{13}$C, Single-Spin Interactions; Best-Fit Results of $^{13}$C MAS NMR Experiments on 1, 1-C1/C4, 1-C2/C3, and 1-U$^{13}$C**

| | $\omega_{iso}^{CS}$ [ppm] | $\delta^{CS}$ [ppm] | $\eta^{CS}$ | $\alpha^{CS}$ [degree] | $\beta^{CS}$ [degree] | $\gamma^{CS}$ [degree] |
|---|---|---|---|---|---|---|
| $^{13}$C1[a] | −172.3 | −67.7 | 1.0 | 90° ± 5° | 67° ± 4° | 10° ± 10° |
| $^{13}$C2[a] | −137.2 | −87.9 | 0.8 | 90° ± 6° | 83° ± 2° | 185° ± 10° |

[a] C1–C4 and C2–C3, respectively, are related by mirror plane symmetry; for corresponding relationships of the $^{13}$C chemical shielding tensor parameters see Experimental.

ods (*19–21*) which permit direct computation of $\gamma_{CR}$-averaged spectra reduce the necessary amount of computing time by about an order of magnitude as compared to the original approach (*18*). Another general major computation-time saver is the choice of smart powder-averaging methods (*22, 23*). Further reductions in computation time by reducing the number of parameters can be achieved by a rigorous exploitation of the symmetry properties of a given spin system.

*Preliminary Elimination of Some Unknowns*

The single-crystal X-ray structure of **1** (*27*) shows that **1** crystallizes in space group *Pbcm*. In this structure the maleate anion is a planar moiety, located on a special crystallographic position such that the O···H···O hydrogen atom (see Scheme 1) resides on a mirror plane, perpendicular to the molecular plane and bisecting the C2═C3 double bond. The crystal structure of **1** provides all interatomic C–C distances and bond angles in the maleate unit (C1–C2, 149.0 pm; C2–C3, 132.9 pm; ∠C1–C2–C3, 130.8°), from which we may calculate the corresponding dipolar coupling constants $b_{ij}$ as well as all Euler angles $\alpha_{ij}^{D}$, $\beta_{ij}^{D}$, and $\gamma_{ij}^{D}$. We can use these values as calculated from the X-ray crystal structure as known and fixed input parameters for spectral lineshape fitting of MAS NMR spectra. Additionally, we may wish to perform iterative fits where these are free fit parameters, and only in the end compare the best-fit parameters with the values calculated from the X-ray crystal structure.

$^{13}$C MAS NMR spectra of **1** (where $^{13}$C is in natural abundance) are in agreement with the molecular symmetry as determined by single-crystal X-ray diffraction. One $^{13}$C resonance for C1/4 ($\omega_{iso}^{CS}$ = −172.3 ppm) and one for C2/3 ($\omega_{iso}^{CS}$ = −137.2 ppm) are observed. There are no further direct clues regarding the structure and geometry of the maleate unit to be retrieved from $^{13}$C MAS NMR spectra of **1,** with $^{13}$C in low natural abundance. However, $^{13}$C MAS NMR spectra of **1** provide magnitudes and asymmetry parameters of the $^{13}$C chemical shielding tensors for C1/4 and C2/3 (see Table 1). In various subsequent iterative lineshape fitting steps, again we can either use these data from $^{13}$C MAS NMR spectra of **1** as fixed input parameters, or for purposes of checking if we would have determined the correct chemical shielding tensor eigenvalues from iterative fitting of $^{13}$C MAS NMR spectra of, e.g., **1-C2/C3** or **1-C1/C4** with $\delta^{CS}$ and $\eta^{CS}$ as free fit parameters.

Solution-state $^{13}$C NMR spectra of **1-U$^{13}$C,** under conditions of $^{1}$H decoupling, represent a $^{13}$C AA′XX′ spin system (in the solution-state NMR sense of denoting the type of a spin system, that is, according to the *J*-coupling paths in the spin system) and allow an independent determination of signs and magnitudes of *J*-coupling constants $J_{iso}^{AA'}$, $J_{iso}^{XX'}$, $J_{iso}^{AX,A'X'}$, and $J_{iso}^{AX',A'X}$ (see Table 2). In subsequent iterative fitting of $^{13}$C MAS NMR spectra of **1-C2/C3, 1-C1/C4,** and **1-U$^{13}$C,** the *J*-coupling data from solution-state NMR served as fixed input parameters, equivalent to the assumption that the various *J*-coupling constants $^{n}J(^{13}C, ^{13}C)$ in the maleate unit in the solid state are similar to those in solution. Owing to their small magnitudes, especially the long-range *J*-coupling constants ($^{3}J(^{13}C1, ^{13}C4)$, $^{2}J(^{13}C1, ^{13}C3)$, $^{2}J(^{13}C2, ^{13}C4)$) appear of minor importance with regard to lineshape simulations of $^{13}$C MAS NMR spectra anyway. If any, then the one-bond *J*-coupling constants ($^{1}J(^{13}C1, ^{13}C2)$, $^{1}J(^{13}C2, ^{13}C3)$) in the $^{13}$C MAS NMR spectra of **1-C2/C3** and **1-U$^{13}$C** may have to be revisited later on.

If, on proceeding to the selectively labeled samples **1-C2/C3** and **1-C1/C4,** we were to use all of the information from X-ray diffraction, solution-state NMR, and $^{13}$C MAS NMR of **1** as fixed parameters, at this stage we would be left with the task of determining six unknown parameters, that is, the six Euler angles $\alpha_i^{CS}$, $\beta_i^{CS}$, and $\gamma_i^{CS}$ ($i$ = 1, 2), for a complete description of the four-$^{13}$C-spin system in **1-U$^{13}$C.**

**TABLE 2**
**$^{13}$C NMR Parameters of 1-U$^{13}$C, Two-Spin Interactions**

| | $J_{iso}$ [Hz][a] | $b_{ij}/2\pi$ [Hz][b] | $\beta^{D}$ [degree][b] | $\gamma^{D}$ [degree][b] |
|---|---|---|---|---|
| $^{13}$C1–$^{13}$C2 | +63 | −2296 | 49.2 | 0 |
| $^{13}$C1–$^{13}$C3 | +1 | −450 | 26.1 | 0 |
| $^{13}$C1–$^{13}$C4 | ±4 | −216 | 0 | 0 |
| $^{13}$C2–$^{13}$C3 | +67 | −3235 | 0 | 0 |
| $^{13}$C2–$^{13}$C4 | +1 | −450 | 153.9 | 0 |
| $^{13}$C3–$^{13}$C4 | +63 | −2296 | 130.8 | 0 |

[a] Determined from solution-state $^{13}$C NMR of **1-U$^{13}$C.**
[b] Calculated from the single-crystal structure of **1** and taking $\Omega_{PC}^{D14} = \Omega_{PC}^{D23} = (0, 0, 0)$.

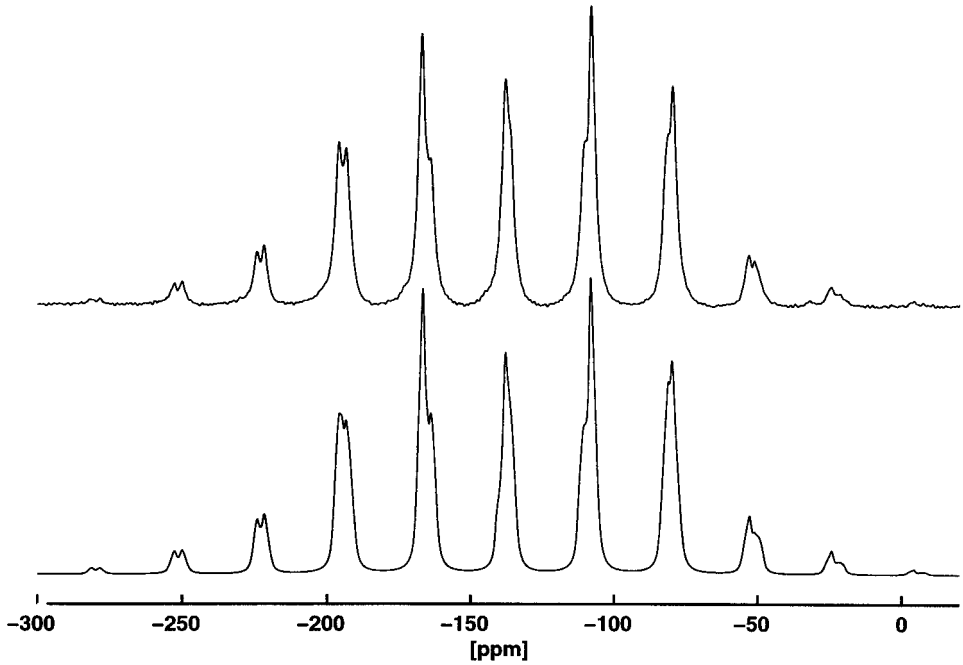


**FIG. 1.** Experimental (top) and simulated (bottom; best-fit parameters, see Table 1) $^{13}$C MAS NMR spectra ($\omega_0/2\pi = -75.5$ MHz; $\omega_r/2\pi = 2146$ Hz) of **1-C2/C3.**

*The $^{13}$C Spin Pairs in* **1-C2/C3** *and* **1-C1/C4**

The C═C carbon sites C2 and C3 in **1** are crystallographically equivalent and related by mirror plane symmetry. The corresponding directly bonded pair of $^{13}$C isotopes in **1-C2/C3** is characterized by a fairly large dipolar coupling constant $b_{23}/2\pi = -3235$ Hz (corresponding to an internuclear $^{13}$C–$^{13}$C distance of 132.9 pm), a sizable anisotropy $\delta_i^{CS} = -87.9$ ppm of the $^{13}$C chemical shielding tensors, an asymmetry parameter $\eta_i^{CS} = 0.8$ ($i = 2, 3$), and the so-called $n = 0$ rotational resonance (*5–8*) condition fulfilled in $^{13}$C MAS NMR spectra at arbitrary MAS frequencies. We find that over a wide range of MAS frequencies and external magnetic field strengths, experimental $^{13}$C MAS NMR spectra of **1-C2/C3** display spectral lineshapes suitable for investigation by iterative lineshape fitting. Figure 1 compares an experimental $^{13}$C MAS NMR spectrum of **1-C2/C3** to the simulated spectrum, corresponding to the best-fit parameters (see Table 1), demonstrating good overall agreement. The iterative fitting procedures yield a well-defined minimum region for the pair of fit parameters $\alpha_2^{CS}$ and $\beta_2^{CS}$ (see contour plot, Fig. 2a), while for reasons of mirror plane symmetry $\gamma_2^{CS}$ cannot be determined from $^{13}$C MAS NMR spectra of **1-C2/C3.** All fit parameters are sensitive parameters as is revealed by scans for individual fit parameters. For instance, the minimum region in the $b_{23}$ scan (Fig. 2b) implies that we would have determined the correct internuclear distance $^{13}$C2–$^{13}$C3 with good precision also without knowing the C2–C3 distance from the single-crystal X-ray structure. Possibilities and limitations regarding the determination of internuclear distances by iterative fitting of $n = 0$ rotational resonance spectra of isolated homonuclear spin pairs are discussed elsewhere in more detail (*16, 17*). Iterative fits of $^{13}$C MAS NMR spectra of **1-C2/C3** define the value of $^1J_{iso}(^{13}C2, ^{13}C3) = +65 \pm 15$ Hz, with a relatively large uncertainty, though in general agreement with the value $^1J_{iso}(^{13}C2, ^{13}C3) = +67$ Hz determined by $^{13}$C solution-state NMR. This justifies our previous assumption that solution-state NMR-derived *J*-coupling constants may be taken as known input parameters for iterative fitting of $^{13}$C MAS NMR spectra, and it demonstrates that nothing would be gained from keeping the various isotropic *J*-coupling constants as free fit parameters, at least not for $^{13}$C MAS NMR spectra of the maleate moiety. The properties of the $^{13}$C spin pair in **1-C2/C3** provide favorable circumstances for the extraction of orientational parameters and/or internuclear distances by iterative lineshape fitting: there are substantial changes of the $^{13}$C spectral lineshapes as a function of the external experimental parameters Larmor and MAS frequency, and there are quite characteristic and substantial changes of the spectral lineshapes as a function of $\alpha_2^{CS}$ and $\beta_2^{CS}$. And yet, in order to avoid local minima, even for a favorable case such as **1-C2/C3,** it is important to rely on several (in particular, several Larmor frequencies) experimental MAS NMR spectra as the basis for the iterative fitting procedure.

Also the two C═O carbon sites C1, C4 in **1** are mutually related by mirror plane symmetry. MAS NMR spectra of the $^{13}$C spin pair in **1-C1/C4** bear some similarities to the $^{13}$C2–

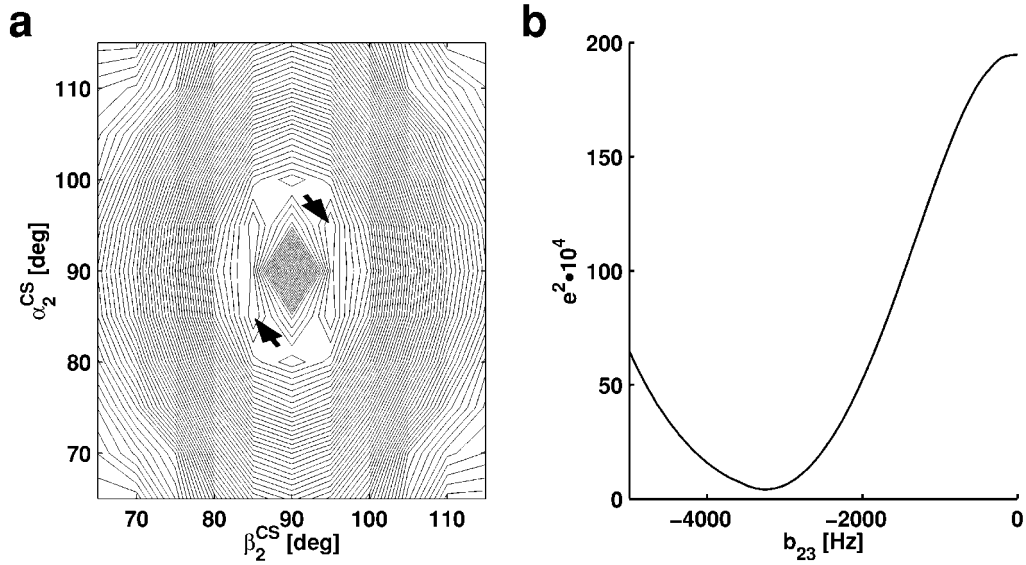


**FIG. 2.** (a) Contour plot of the error plane, calculated for pair of fit parameters $\alpha_2^{CS}$ and $\beta_2^{CS}$; the arrows indicate the (symmetry-related) minimum regions, and contours are drawn at integer multiples of the minimum value; (b) error scan for fit parameter $b_{23}$. Calculations are based on $^{13}$C MAS NMR spectra of **1-C2/C3** obtained at $\omega_0/2\pi = -75.5$ MHz and $\omega_r/2\pi = 2146$ Hz as shown in Fig. 1.

$^{13}$C3 case in **1-C2/C3** (again, $n = 0$ rotational resonance condition fulfilled, sizable anisotropy of the $^{13}$C chemical shielding tensors $\delta_i^{CS} = -67.7$ ppm with an asymmetry parameter $\eta_i^{CS} = 1.0$ ($i = 1, 4$)), as well as some dissimilarities (a much smaller dipolar coupling constant $b_{14}/2\pi = -216$ Hz, corresponding to an internuclear C1–C4 distance of 327.6 pm, and a very small $J$-coupling constant $|^3J_{iso}(^{13}C1, ^{13}C4)| = 4$ Hz, according to solution-state $^{13}$C NMR). Given the small value $b_{14}/2\pi = -216$ Hz, not unexpectedly, line-broadening and splitting effects are less characteristic and spectral lineshape changes as a function of external experimental parameters in $^{13}$C MAS NMR spectra of **1-C1/C4** are less distinct than those for **1-C2/C3.** Despite these less favorable circumstances, there are some characteristic spectral lineshape features also in $^{13}$C MAS NMR spectra of **1-C1/C4.** Figure 3 compares an experimental to the corresponding best-fit simulated $^{13}$C MAS NMR spectrum of **1-C1/C4.** The sensitivity of the fit parameters $\alpha_1^{CS}$ and $\beta_1^{CS}$ is considerably less than that for the $^{13}$C spin pair in **1-C2/C3** (see Fig. 2a for comparison). It becomes more important to engage a larger number of different experimental $^{13}$C MAS NMR spectra of **1-C1/C4** in the iterative lineshape fitting procedure. Figure 4a depicts contour plots of the error planes for the two fit parameters $\alpha_1^{CS}$ and $\beta_1^{CS}$ as determined from three different $^{13}$C MAS NMR spectra of **1-C1/C4** (Fig. 4a, (i)–(iii)), as well as the unweighted sum of these three contour plots (Fig. 4a, (iv)). According to these contour plots, $\alpha_1^{CS} = 90° \pm 5°$ is reasonably well defined, despite limited sensitivity. The situation for $\beta_1^{CS}$ is less clear: while contour plots (ii) and (iii) leave some ambiguity, that is, two minimum regions near $\beta_1^{CS} = 55°$ and $\beta_1^{CS} = 75°$, contour plots (i) and (iv) tend to indicate preference for the minimum region near $\beta_1^{CS} = 75°$. Neither choosing the minimum region near $\beta_1^{CS} = 75°$ as the final solution nor settling the issue by accepting a broad minimum region $\beta_1^{CS} = 65° \pm 15°$ is a particularly satisfying solution, given the limited sensitivity of these fits. Owing to the small dipolar coupling constant $b_{14}/2\pi = -216$ Hz, little can be done about this remaining uncertainty for $\beta_1^{CS}$ from consideration of $^{13}$C MAS NMR spectra of **1-C1/C4** alone. For the moment we may leave the question open and will return to the $\beta_1^{CS}$ issue when discussing $^{13}$C MAS NMR spectra of **1-U$^{13}$C:** the presence of a sizable dipolar coupling constant $b_{12}/2\pi = -2296$ Hz in the fully $^{13}$C-enriched maleate moiety provides another option for determining $\beta_1^{CS}$. The scan shown in Fig. 4b characterizes $b_{14}$, despite its small magnitude, as a sensitive fit parameter which would have provided the correct internuclear C1–C4 distance also in the absence of single-crystal X-ray diffraction information. The $^{13}$C spin pair in **1-C1/C4** obviously represents a case close to the upper limit of tolerable internuclear carbon–carbon distances (here, 327.6 pm) when aiming at the determination of $^{13}$C chemical shielding tensor orientations from spectral lineshapes of $n = 0$ rotational resonance $^{13}$C MAS NMR spectra.

The $n = 0$ rotational resonance condition encountered for each of the two selectively $^{13}$C-enriched spin-pair samples **1-C2/C3** and **1-C1/C4** is a rather special and favorable condition with regard to spectral lineshape simulations. For the $n = 0$ rotational resonance condition we can ignore the $^1$H-decoupling performance to a certain extent, since both sites involved are equally affected by good (or poor) decoupling performance. As long as the ("relative") heteronuclear decoupling performance is good enough to grant sufficient sensitivity of the iterative fitting procedures for all parameters of the respective homonuclear $^{13}$C spin pair (other than line broadening), we do not have to worry too much about the "absolute" $^1$H-

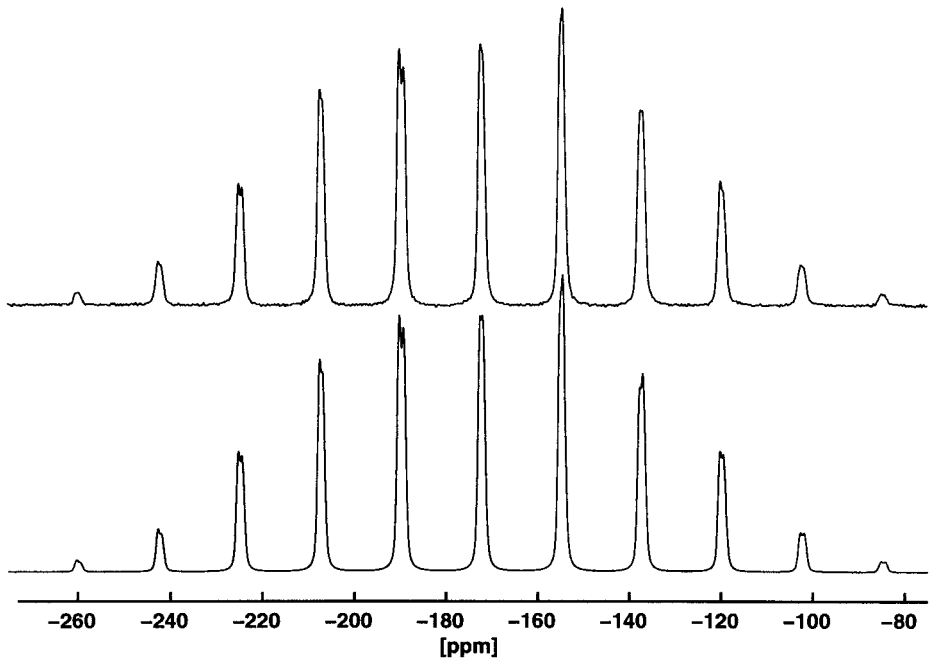


**FIG. 3.** Experimental (top) and simulated (bottom; best-fit parameters, see Table 1) $^{13}$C MAS NMR spectra ($\omega_0/2\pi = -50.3$ MHz; $\omega_r/2\pi = 881$ Hz) of **1-C1/C4.**

decoupling performance. Figures 1–4 illustrate that a regime of sufficiently good $^1$H-decoupling performance is reached for the $n = 0$ rotational resonance condition in the selectively $^{13}$C-enriched samples **1-C2/C3** and **1-C1/C4** with cw $^1$H on-resonance decoupling fields of about 85 kHz at modest external magnetic field strengths $B_0 = 4.7$ T and $B_0 = 7.0$ T. Apart from a so far remaining ambiguity for $\beta_1^{CS}$, all fit parameters for the $^{13}$C spin pairs in **1-C2/C3** and **1-C1/C4,** $\alpha_i^{CS}$, $\beta_i^{CS}$, as well as $b_{ij}$, are sensitive fit parameters. The fairly silent role of the $^1$H spins as a generally welcome, time-saving source of observable $^{13}$C magnetization by way of Hartmann–Hahn cross polarization, but as an otherwise negligible quantity during

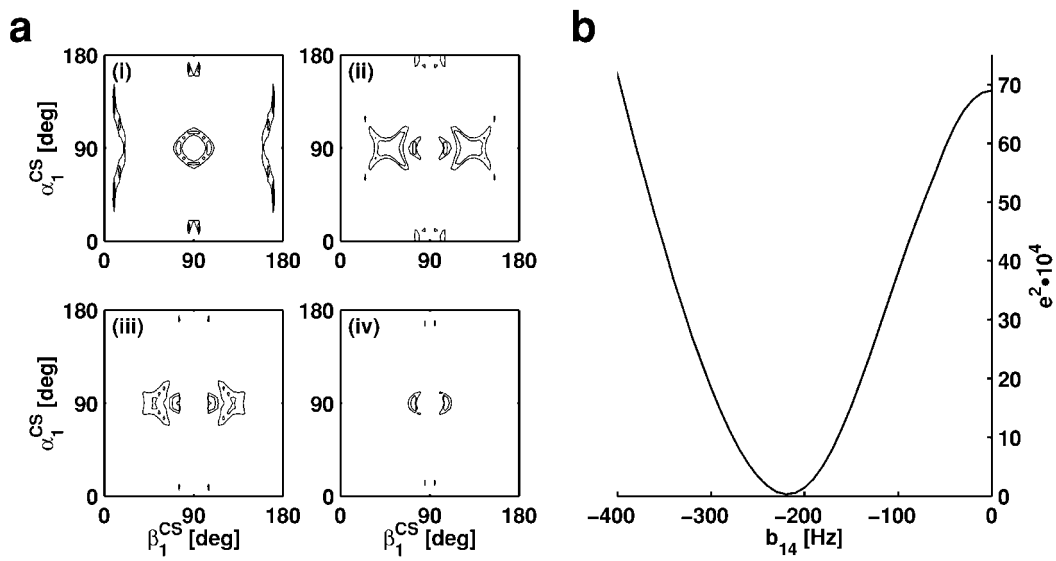


**FIG. 4.** (a) Contour plots of error planes for the two fit parameters $\alpha_1^{CS}$ and $\beta_1^{CS}$ from three different $^{13}$C MAS NMR spectra of **1-C1/C4** ((i)–(iii)) and the unweighted sum of these three contour plots (iv); only contour levels at twice and three times the minimum value are drawn; (b) error scan for fit parameter $b_{14}$. Calculations are based on $^{13}$C MAS NMR spectra of **1-C1/C4** obtained at $\omega_0/2\pi = -75.5$ MHz; $\omega_r/2\pi = 2099$ Hz (a(i)), $\omega_0/2\pi = -75.5$ MHz; $\omega_r/2\pi = 1163$ Hz (a(ii)), $\omega_0/2\pi = -50.3$ MHz; $\omega_r/2\pi = 881$ (a(iii)), and $\omega_0/2\pi = -50.3$ MHz; $\omega_r/2\pi = 881$ Hz (b).

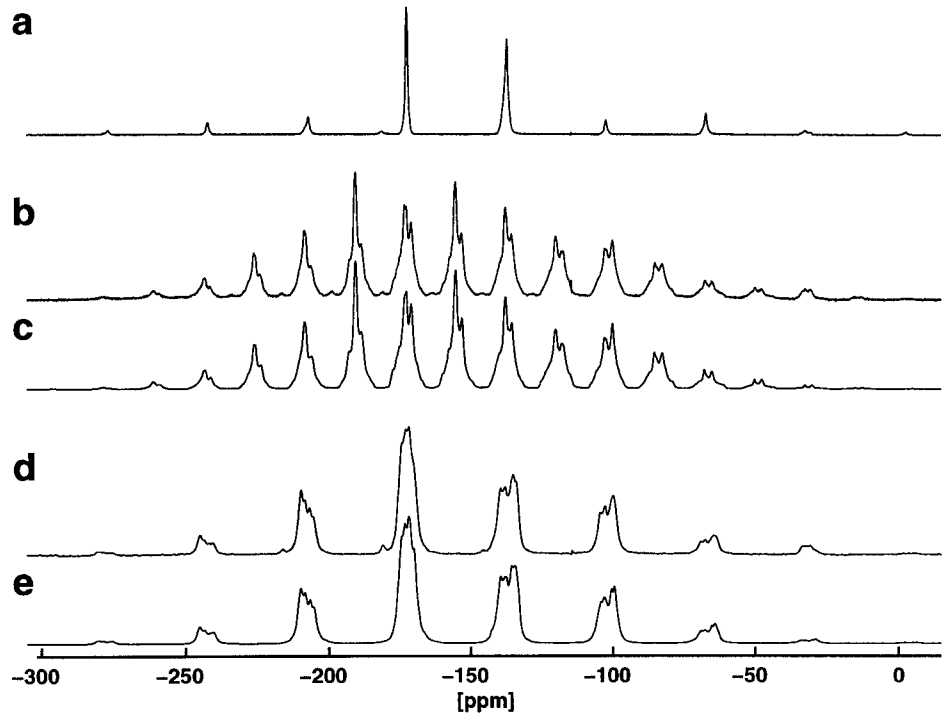


**FIG. 5.** (a, b, d) Experimental $^{13}$C MAS NMR spectra ($\omega_0/2\pi = -125.8$ MHz; TPPM decoupling (*23*)) of **1-U$^{13}$C,** obtained at $\omega_r/2\pi = 8776$ Hz (a), with CP excitation, at the $n = 2$ rotational resonance condition for the $^{13}$C1/4 and $^{13}$C2/3 resonances, $\omega_r/2\pi = 2212$ Hz (b), and with SP excitation, at the $n = 1$ rotational resonance condition, $\omega_r/2\pi = 4425$ Hz (d); (c) the corresponding best-fit (see Table 1) simulated $n = 2$ rotational resonance spectrum; (e) the best-fit simulated $n = 1$ rotational resonance spectrum.

acquisition of the $^{13}$C free induction decay by way of $^{1}$H decoupling, changes as soon as we step away from the $n = 0$ rotational resonance condition. Moving on from the pairwise selectively $^{13}$C-enriched samples **1-C2/C3** and **1-C1/C4** to the four-$^{13}$C-spin system in **1-U$^{13}$C** includes the step from $n = 0$ to $n = 1, 2$ rotational resonance conditions. Apart from some remaining ambiguity concerning $\beta_1^{CS}$, at this stage only two parameters, that is, the Euler angles $\gamma_i^{CS}$ ($i = 1, 2$), remain to be determined.

### *The Four-$^{13}$C-Spin System in* **1-U$^{13}$C**

An isotropic $^{13}$C chemical shielding difference of 35.1 ppm between the $^{13}$C1/4 and $^{13}$C2/3 resonances renders $^{13}$C MAS NMR spectra of **1-U$^{13}$C,** obtained at *arbitrary* MAS frequencies, unsuitable for determining the remaining unknown parameters $\gamma_i^{CS}$ ($i = 1, 2$). However, this 35.1 ppm difference makes $n = 1, 2$ rotational resonance (*1–7*) conditions (where $\omega_{iso}^{\Delta} = n\omega_r$ and $n$ is a small integer) for these two pairs of resonances accessible over a fairly large range of external magnetic field strengths. Relatively large chemical shielding anisotropies $\delta_i^{CS}$ ($i = 1$–4) and the $n = 0$ rotational resonance condition for the $^{13}$C1/4 and $^{13}$C2/3 pairs maintained at all MAS frequencies provide good starting conditions for further exploitation of $n = 1, 2$ rotational resonance lineshapes in $^{13}$C MAS NMR spectra of **1-U$^{13}$C** in order to establish the so far missing links between the $^{13}$C1/4 and $^{13}$C2/3 subsets of the spin system.

In order to avoid yet another fit parameter, that is, the relative intensities of the $^{13}$C1/4 and $^{13}$C2/3 resonances, one may wish to choose $^{13}$C single-pulse excitation rather than cross polarization (CP) to record $n = 1, 2$ rotational resonance $^{13}$C MAS NMR spectra of **1-U$^{13}$C.** Of course, single-pulse (SP) excitation is not a particularly realistic approach for compounds other than model compounds such as **1-U$^{13}$C,** it merely offers convenience of computation. There is no fundamental reason to avoid CP where CP is possible and desirable for experimental (signal-to-noise) reasons, except that CP-based spectral lineshapes require an additional fit parameter, "relative intensities." We have used both CP and SP excitation to record experimental $^{13}$C MAS NMR spectra of **1-U$^{13}$C** and find no negative side effects of CP-generated experimental spectra on the iterative fitting procedures. Figures 5a, 5b, and 5d display three experimental $^{13}$C MAS NMR spectra (Larmor frequency $\omega_0/2\pi = -125.8$ MHz) of **1-U$^{13}$C,** one obtained at high spinning frequency (Fig. 5a, $\omega_r/2\pi = 8776$ Hz), one obtained at the $n = 2$ rotational resonance condition for the $^{13}$C1/4 and $^{13}$C2/3 resonances (Fig. 5b, $\omega_r/2\pi = 2212$ Hz), and one obtained at the $n = 1$ rotational resonance condition (Fig. 5d, $\omega_r/2\pi = 4425$ Hz). In Figs. 5c and 5e we show the corresponding best-fit simulated $n = 2, 1$ rotational resonance $^{13}$C MAS

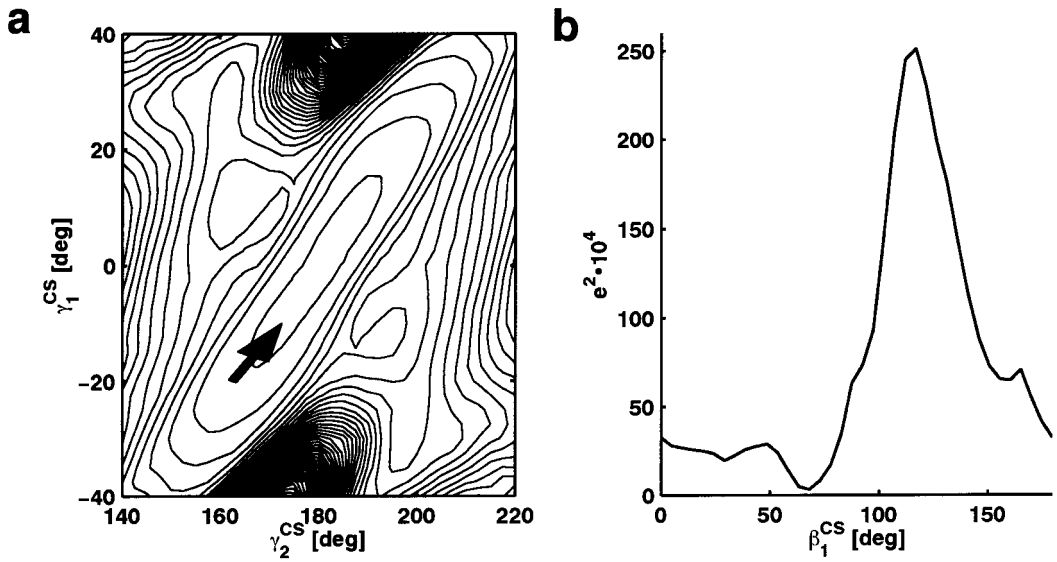


**FIG. 6.** (a) Contour plot of the error plane for the two fit parameters $\gamma_1^{CS}$ and $\gamma_2^{CS}$; contours are drawn at integer multiples of the minimum value and the arrow indicates the minimum region; (b) error scan for fit parameter $\beta_1^{CS}$. Calculations are based on the experimental spectrum shown in Fig. 5b. Note that for reasons of symmetry the minimum region in the contour plot in (a) appears twice as large as is physically meaningful.

NMR spectra for **1-U$^{13}$C.** Figures 5c and 5e seemingly complete our task to determine the two remaining unknown Euler angles $\gamma_i^{CS}$ ($i = 1, 2$) as well as to reconsider a more precise determination of $\beta_1^{CS}$ than was possible to derive from $n = 0$ rotational resonance $^{13}$C MAS NMR spectra of **1-C1/C4.** A contour plot of the error planes for the two fit parameters $\gamma_1^{CS}$ and $\gamma_2^{CS}$ (Fig. 6a) and a $\beta_1^{CS}$ scan (Fig. 6b) confirm this statement: $\gamma_1^{CS} = 10° \pm 10°$, $\gamma_2^{CS} = 185° \pm 10°$, and $\beta_1^{CS} = 67° \pm 4°$ are well defined. At this stage, basically all parameters of the $^{13}$C spin system in **1-U$^{13}$C** are known, which enables us to examine next if and how well we could have determined all these parameters, had only the four-$^{13}$C-spin system been available.

Before doing so, we need to address possible pitfalls and potentially problematic steps in the iterative lineshape fitting approach. The first point of concern is actually the sample itself, as we have used the fully $^{13}$C-labeled, nondilute version of monoammonium maleate, **1-U$^{13}$C.** For this particular compound one can afford this choice of sample: the alternate layer structure of solid monoammonium maleate results in good spatial separation between neighbored maleate units in the three-dimensional structure (*27*). From a comparison of spectral lineshapes for **1-U$^{13}$C** and for a dilute, 10% labeled sample, **1-U$^{13}$C in 1** (spectra not shown), we have come to the conclusion that for this particular compound more severe errors would be introduced into the lineshape fitting procedure by subtracting the natural abundance $^{13}$C background from the dilute sample than by ignoring intermolecular dipolar coupling in the fully $^{13}$C-labeled sample **1-U$^{13}$C.** This is *not* a general recommendation to ignore intermolecular dipolar coupling in fully $^{13}$C-labeled samples; here we just take advantage of a special (and rather convenient) structural property of solid monoammonium maleate. Another point of concern with iterative lineshape fitting approaches to rotational resonance $^{13}$C MAS NMR spectra relates to the simulation procedure itself. A basic underlying assumption made (see Eq. [1]) is perfect isolation of the $^{13}$C spin system from surrounding $^{1}$H spins. In practice, the $^{1}$H-decoupling performance may be less than ideal. Indeed, anomalous lineshapes have been repeatedly observed for isolated $^{13}$C spin pairs under rotational resonance and cw $^{1}$H-decoupling conditions. Very recently, these anomalous lineshapes have been explained in terms of differential transverse relaxation, brought about by less than perfect $^{1}$H decoupling (*31*). One may not be able to completely eliminate such $^{1}$H-decoupling problems from experimental spectra, but we can considerably lessen unwanted lineshape artifacts by taking a few precautions when choosing our experimental conditions. Theory predicts (i) increasingly disturbed rotational resonance $^{13}$C spectral lineshapes from nonperfect $^{1}$H cw decoupling to occur at higher external magnetic field strengths and/or higher MAS frequencies, and (ii) the most prominent anomalous/additional lineshape features to appear in the centerband spectral region of the nonprotonated $^{13}$C site (*31*). In practice we find that cw $^{1}$H decoupling (up to 100 kHz decoupling field) performs unsatisfactorily for **1-U$^{13}$C** at all external magnetic field strengths used (4.7 to 11.7 T) and fails to yield undisturbed experimental $n = 1, 2$ rotational resonance $^{13}$C NMR lineshapes. Improved heteronuclear decoupling schemes, such as TPPM (*24*), turn out to perform well and yield reliable $^{13}$C $n = 1, 2$ rotational resonance spectral lineshapes for **1-U$^{13}$C** even at $B_0 = 11.7$ T. With these considerations in mind we return to Fig. 5 for closer inspection. All experimental $^{13}$C spectra shown in Fig. 5 were obtained with TPPM (*24*) decoupling and a $^{1}$H-decoupling field of 105

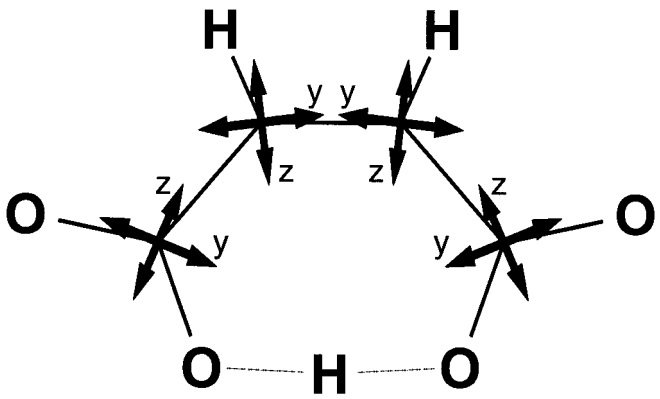


**FIG. 7.** Schematic illustration of the $^{13}$C chemical shielding tensor orientations in the molecular frame of the maleate moiety. Shown is the projection of the $\omega_{yy}$ and $\omega_{zz}$ components of the $^{13}$C1/4 and $^{13}$C2/3 shielding tensors onto the molecular plane. The most shielded components $\omega_{xx}$ of both tensors are oriented nearly perpendicular ($\gamma_1^{CS} = 10° \pm 10°$, $\gamma_2^{CS} = 185° \pm 10°$) to the molecular plane.

kHz. Under these experimental conditions we find excellent agreement between experimental and best-fit simulated $n = 2$ rotational resonance spectral lineshapes (see Figs. 5b and 5c) and close to excellent agreement for the $n = 1$ rotational resonance condition (see Figs. 5d and 5e). In accordance with theoretical predictions (*31*) a *very* minor additional spectral feature occurs in the $n = 1$ experimental rotational resonance spectrum of **1-U$^{13}$C** in the middle of the centerband region of the $^{13}$C1/4 resonance, while there is virtually no difference between best-fit simulated and experimental lineshapes in the $n = 2$ rotational resonance spectra of **1-U$^{13}$C.** Fitting these experimental $n = 2$ or $n = 1$ rotational resonance $^{13}$C ($\omega_0/2\pi = -125.8$ MHz) data, as well as $n = 1$ rotational resonance $^{13}$C spectra of **1-U$^{13}$C** obtained at $\omega_0/2\pi = -100.6$ MHz with TPPM decoupling (spectra not shown), independently converges to identical best-fit parameters (see Table 1).

After this excursion to identify and address potential sources of difficulties, we return to the complete, best-fit set of parameters of the $^{13}$C spin system in **1-U$^{13}$C** (see Table 1), and inspect how these parameters relate to the molecular geometry of the maleate anion and to known single-crystal $^{13}$C NMR data of related compounds. The (best-fit) orientations of the $^{13}$C chemical shielding tensors in the maleate moiety are illustrated in Fig. 7. The most shielded (here, $\omega_{xx}$) components of both the C = (C2/3) and C═O (C1/4) $^{13}$C chemical shielding tensors are nearly perpendicular to the molecular plane. For C2/3 the intermediate $^{13}$C chemical shielding tensor component is oriented at an angle of 23° to the direction of the C2═C3 bond, while the least shielded component is oriented at an angle of 18° to the C–H bond direction. For C1/4 the intermediate $^{13}$C chemical shielding tensor components are oriented near the C═O bond directions (at an angle of 11°) and the least shielded components deviate by 20° from the C1–C2 or C3–C4 bond directions, respectively. These orientational parameters for the maleate moiety are in very good general agreement with the results of previous $^{13}$C NMR studies on oriented single crystals of related compounds such as maleic anhydride (*32*), malonic acid (*33*), dimedone (*34*), tetraacetylethane (*35*), and Meldrum's acid (*36*). In common with our results, these single-crystal $^{13}$C NMR studies reveal trends in $^{13}$C chemical shielding tensor orientations in the molecular frame, more or less near major chemical bond directions, including trends in deviations from these bond directions: it occurs very rarely that $^{13}$C chemical shielding tensor components and bond directions are precisely collinear. Such orientational deviations from the major molecular chemical bond directions may appear to be of minor importance and, in fact, have led to the widespread use and concept of "typical" $^{13}$C shielding tensor orientations where coincidence rather than vicinity of molecular bond directions and chemical shielding tensor components is assumed. For instance, when aiming at the determination of molecular conformation based on assumed typical $^{13}$C chemical shielding tensor orientations, this may easily account for uncertainties of 20°, or even more, in estimations of molecular conformational parameters. The pronounced influence of relatively small deviations of the $^{13}$C chemical shielding tensor orientations from typical orientations for the maleate moiety (typical orientations $^{13}$C2/3, $\omega_{yy}$ taken as collinear with the C2═C3 bond direction, and $^{13}$C1/4, $\omega_{yy}$ taken as collinear with the C1/4═O bond direction) on lineshapes of $^{13}$C MAS NMR spectra of **1-U$^{13}$C** is illustrated in Fig. 8: there are major lineshape discrepancies between the experimentally observed and the simulated spectrum when assuming these typical orientations. Such discrepancies, when operating in the "typical-orientation-assumption mode," may lead to much reduced sensitivity of various kinds of simulation and fit procedures and may result in inaccurate or even wrong parameters in a much more general context. We will return to this aspect below.

Finally, we will now assume that only the four-$^{13}$C-spin system **1-U$^{13}$C** is available and will examine two limiting model situations in more detail. For the first model situation we assume known carbon–carbon distances and bond angles, with all $^{13}$C chemical shielding tensor orientations in the molecule to be determined simultaneously. From a molecular structure point of view, this task could be described as equivalent to determining molecular conformation from chemical shielding tensor orientations. Our second model situation will examine how well all intramolecular dipolar coupling constants $b_{ij}$ would have been determined simultaneously when using different chemical shielding tensor orientations as fixed parameters in the fitting procedure. In terms of molecular structure, this situation corresponds to deriving the geometry of a molecule or molecular fragment, i.e., internuclear distances and bond angles, from dipolar coupling tensors.

Our first model situation takes the best-fit parameters as fixed input, except that the chemical shielding tensor orientations are initially chosen to correspond to the typical orientations (see simulated spectrum in Fig. 8) and all six angles defining the orientation of the chemical shielding tensors in

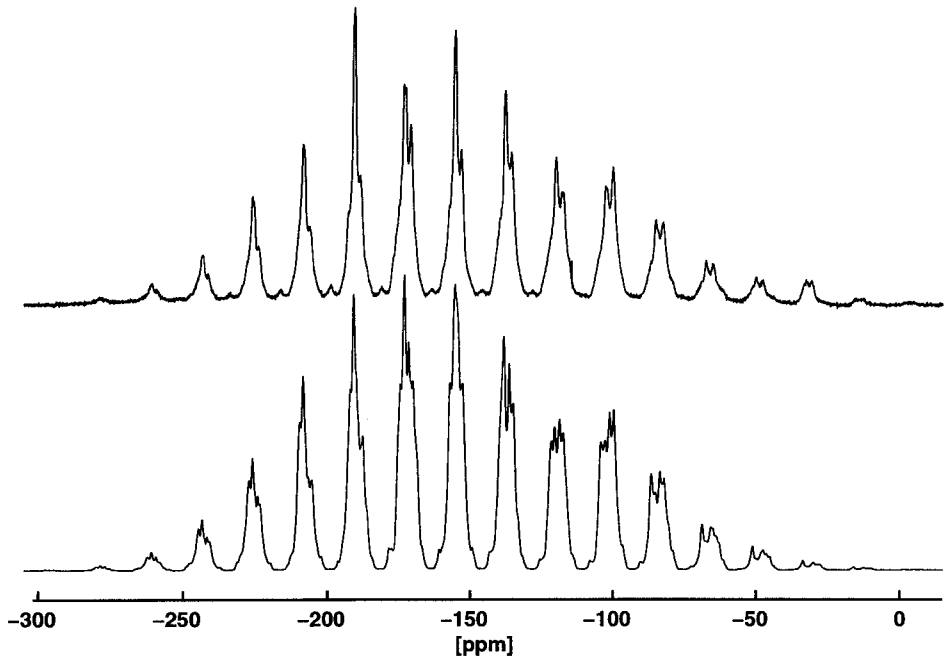


**FIG. 8.** Experimental (top) and simulated (bottom) $^{13}$C MAS NMR spectra of **1-U$^{13}$C.** The experimental spectrum is identical to the spectrum shown in Fig. 5b. The simulated spectrum employs all best-fit parameters from Table 1, except that $\alpha_i^{CS}$, $\beta_i^{CS}$, and $\gamma_i^{CS}$ have been adjusted according to a "typical" orientation ($\omega_{yy}^{2,3}$ collinear with the C2═C3 bond direction; $\omega_{yy}^{1,4}$ collinear with the C1/4═O bond direction; $\omega_{xx}^{ij}$ perpendicular to the molecular plane). Note that these relatively minor changes in chemical shielding tensor orientations result in major discrepancies between experimental and simulated spectral lineshapes.

**1-U$^{13}$C** are free fit parameters. Using the experimental $n = 2$ rotational resonance spectrum of **1-U$^{13}$C** shown in Fig. 8, this multiparameter fit smoothly converges to yield chemical shielding tensor orientations identical to those we had previously determined in a stepwise manner, with two- and three-parameter fits at a time, by taking advantage of the pairwise $^{13}$C-labeled samples **1-C1/C4** and **1-C2/C3** upon approaching the four-$^{13}$C-spin system in **1-U$^{13}$C.** In other words, this model situation would have provided very accurate information on molecular conformational parameters.

Our second model situation essentially probes how accurately we would have determined bond lengths and the geometry of the maleate moiety from multiparameter fits of rotational resonance spectra of **1-U$^{13}$C** when using different, fixed $^{13}$C chemical shielding tensor orientations while searching for the values $b_{ij}$. First, we examine a situation where the fixed input parameters are the best-fit values (including the correct orientation of the $^{13}$C chemical shielding tensors), except that the initial values of all dipolar coupling constants $b_{ij}$ are deliberately misadjusted such that the corresponding internuclear distances are wrong by 20%, and all values $b_{ij}$ are free fit parameters. The result of this iterative fit is quantitative agreement of all internuclear distances C1–C2 and C2–C3 (within less than 1%) and C1–C3 and C1–C4 (within less than 4%) with the internuclear distances determined by single-crystal X-ray diffraction. Next, we repeat this iterative-fit scenario with all $b_{ij}$ as free fit parameters and an identical $b_{ij}$ misadjustment as initial input. However, this time we fix the orientation of the four $^{13}$C chemical shielding tensors to the above-mentioned typical orientations. Note that for the maleate moiety in **1-U$^{13}$C** this requires only a minor change in chemical shielding tensor orientations. The best-fit result from this typical orientations scenario is dramatically inaccurate internuclear distances. For instance, the best-fit results now over-estimate the C1–C4 internuclear distance by about 50%, and the C1–C2 and C1–C3 distances are wrong by about 10–15%:

| Distances [pm]: | C1–C2 | C1–C3 | C1–C4 | C2–C3 |
|---|---|---|---|---|
| From X-ray diffraction | 149.0 | 256.4 | 327.6 | 132.9 |
| From "typical orientations" fit | 158.9 | 289.9 | 475.5 | 123.5 |
| From "correct orientations" fit | 148.3 | 265.5 | 340.4 | 134.1 |

Of course, for **1-U$^{13}$C** we know that the C2–C3 double bond is in a *cis* configuration. For a more realistic application situation, the overestimated C1–C4 distance from the typical orientation fit result would probably have caused a complete misinterpretation of the molecular structure as a *trans* configuration at the C═C bond. In contrast to this typical orientation scenario, iterative fits employing the correct $^{13}$C chemical shielding tensor orientations deliver carbon–carbon bond distances from the four-$^{13}$C-spin system in **1-U$^{13}$C** in good agreement with the values determined by single-crystal X-ray diffraction.

## CONCLUSIONS

Our study of **1-U$^{13}$C** demonstrates that efficient and numerically exact lineshape simulation methods can handle a spin system composed of four dipolar-coupled spin-$\frac{1}{2}$ nuclei under MAS conditions in a reliable and accurate manner, provided that chemical shielding tensor orientations are properly taken into account and optimized $^{1}$H-decoupling techniques (where applicable) are employed. The exploitation of various rotational resonance conditions in MAS NMR studies of homonuclear spin systems, as we have employed here for the study of the four-$^{13}$C-spin system in **1-U$^{13}$C,** is only one of many experimental circumstances where this is relevant. Being able to "afford" to include magnitudes and orientations of *all* interaction tensors within an $n$-spin system also for $n > 2$ in simulations is important for the careful analysis of experimental MAS NMR data from a large variety of homo- and heteronuclear dipolar recoupling techniques (*5, 6*).

In addition, the four-$^{13}$C-spin system in **1-U$^{13}$C** illustrates the dangers of using "typical" chemical shielding tensor parameters when aiming at the determination of internuclear distances from, e.g., $^{13}$C rotational resonance NMR experiments. Our results show that assuming chemical shielding tensor orientations with only limited accuracy, within about 20° of the true orientation, leads to unacceptable errors in internuclear distances derived from MAS NMR experiments. Since contemporary trends in MAS NMR include the use of increasingly higher external magnetic field strengths, chemical shielding tensor parameters will play an increasingly important role. Accordingly, magnitudes as well as orientations of chemical shielding tensors need to be more actively considered.

## ACKNOWLEDGMENTS

Support of our work by the Deutsche Forschungsgemeinschaft, the Fonds der Chemischen Industrie, and the Swedish Natural Science Research Foundation is gratefully acknowledged. We thank H. Förster and S. Steuernagel, Bruker Analytik GmbH, Rheinstetten, for recording $^{13}$C MAS NMR spectra on the DSX 400 and DSX 500 NMR spectrometers, and B. Wrackmeyer, Bayreuth, for providing solution-state $^{13}$C NMR spectra of **1-U$^{13}$C.** We thank M. H. Levitt, Stockholm, for discussions and for sharing unpublished results.

## REFERENCES

1. M. H. Levitt, D. P. Raleigh, F. Creuzet, and R. G. Griffin, Theory and simulations of homonuclear spin pairs in rotating solids, *J. Chem. Phys.* **92,** 6347–6364 (1990).
2. A. Schmidt and S. Vega, The Floquet theory of nuclear magnetic resonance spectroscopy of single spins and dipolar coupled spin pairs in rotating solids, *J. Chem. Phys.* **96,** 2655–2680 (1992).
3. T. Nakai and C. A. McDowell, An analysis of NMR spinning sidebands of homonuclear two-spin systems using Floquet theory, *Mol. Phys.* **77,** 569–584 (1992).
4. T. Nakai and C. A. McDowell, Application of Floquet theory to the nuclear magnetic resonance spectra of homonuclear two-spin systems in rotating solids, *J. Chem. Phys.* **96,** 3452–3466 (1992).
5. A. E. Bennett, R. G. Griffin, and S. Vega, Recoupling of homo- and heteronuclear dipolar interactions in rotating solids, *in* "Solid-State NMR IV: Methods and Applications of Solid-State NMR, Vol. 33, NMR Basic Principles and Progress" (B. Blümich, Ed.), pp. 1–78, Springer-Verlag, Berlin (1994).
6. S. Dusold and A. Sebald, Dipolar recoupling under magic-angle-spinning conditions, *in* "Annual Reports on NMR Spectroscopy" (G. Webb, Ed.), Vol. 41, Academic Press, London (2000).
7. D. P. Raleigh, M. H. Levitt, and R. G. Griffin, Rotational resonance in solid state NMR, *Chem. Phys. Lett.* **146,** 71–76 (1988).
8. A. Kubo and C. A. McDowell, One- and two-dimensional $^{31}$P cross-polarization magic-angle-spinning nuclear magnetic resonance studies on two-spin systems with homonuclear dipolar and *J* coupling, *J. Chem. Phys.* **92,** 7156–7170 (1990).
9. N. C. Nielsen, F. Creuzet, R. G. Griffin, and M. H. Levitt, Enhanced double-quantum nuclear magnetic resonance in spinning solids at rotational resonance, *J. Chem. Phys.* **96,** 5668–5677 (1992).
10. Y. Tomita, E. J. O'Connor, and A. McDermott, A method for dihedral angle measurement in solids: Rotational resonance NMR of a transition-state inhibitor of triose phosphate isomerase, *J. Am. Chem. Soc.* **116,** 8766–8771 (1994).
11. R. Challoner and A. Sebald, A double-quantum $^{119}$Sn rotational-resonance study, *J. Magn. Reson. A* **122,** 85–89 (1996).
12. P. R. Costa, B. Sun, and R. G. Griffin, Rotational resonance tickling: Accurate internuclear distance measurement in solids, *J. Am. Chem. Soc.* **119,** 10821–19830 (1997).
13. G. Wu, B. Sun, R. E. Wasylishen, and R. G. Griffin, Spinning sidebands in slow-magic-angle-spinning NMR spectra arising from tightly *J*-coupled spin pairs, *J. Magn. Reson.* **124,** 366–371 (1997).
14. S. Dusold, J. Kümmerlen, and A. Sebald, A $^{31}$P NMR study of solid compounds $M_xP_2O_7$, *J. Phys. Chem. A* **101,** 5895–5900 (1997).
15. S. Dusold, E. Klaus, A. Sebald, M. Bak, and N. C. Nielsen, Magnitudes and relative orientations of chemical shielding, dipolar, and *J* coupling tensors for isolated $^{31}$P–$^{31}$P spin pairs determined by iterative fitting of $^{31}$P MAS NMR spectra, *J. Am. Chem. Soc.* **119,** 7121–7129 (1997).
16. S. Dusold, W. Milius, and A. Sebald, Iterative lineshape fitting of MAS NMR spectra: A tool to investigate homonuclear *J* coupling in isolated spin pairs, *J. Magn. Reson.* **135,** 500–513 (1998).
17. S. Dusold and A. Sebald, Determination of magnitudes and orientations of interaction tensors from MAS NMR spectra of isolated three-spin systems ABX, *Mol. Phys.* **95,** 1237–1245 (1998).
18. M. Edén, Y. K. Lee, and M. H. Levitt, Efficient simulation of periodic problems in NMR: Application to decoupling and rotational resonance, *J. Magn. Reson. A* **120,** 56–71 (1996).
19. T. Charpentier, C. Fermon, and J. Virlet, Efficient time propagation technique for MAS NMR simulation: Application to quadrupolar nuclei, *J. Magn. Reson.* **132,** 181–190 (1998).
20. M. Hohwy, H. Bildsoe, H. J. Jakobsen, and N. C. Nielsen, Efficient spectral simulations in NMR of rotating solids. The $\gamma$-COMPUTE algorithm, *J. Magn. Reson.* **136,** 6–14 (1999).
21. M. H. Levitt and M. Edén, Numerical simulation of periodic NMR problems: Fast calculation of carousel averages, *Mol. Phys.* **95,** 879–890 (1998).
22. M. Bak and N. C. Nielsen, REPULSION, a novel approach to efficient powder averaging in solid-state NMR, *J. Magn. Reson.* **125,** 132–139 (1997).
23. M. Edén and M. H. Levitt, Computation of orientational averages in solid state NMR by Gaussian spherical quadrature, *J. Magn. Reson.* **132,** 220–239 (1998).

*24.* A. E. Bennett, C. M. Rienstra, M. Auger, K. V. Lakshmi, and R. G. Griffin, Heteronuclear decoupling in rotating solids, *J. Chem. Phys.* **103,** 6951–6958 (1995).

*25.* M. H. Levitt, The signs of frequencies and phases in NMR, *J. Magn. Reson.* **126,** 164–182 (1997).

*26.* U. Haeberlen, High resolution NMR in solids. Selective averaging, *in* "Advances in Magnetic Resonance" (J. S. Waugh, Ed.), Supplement 1, Academic Press, New York (1976).

*27.* L. Golic and I. Leban, The crystal structure of ammonium hydrogen maleate, *Croat. Chim. Acta* **55,** 41–45 (1982).

*28.* S. A. Smith, T. O. Levante, B. H. Meier, and R. R. Ernst, Computer simulations in magnetic resonance. An object oriented programming approach, *J. Magn. Reson. A* **106,** 75–105 (1994).

*29.* F. James and M. Roos, MINUIT computer code, Program D-506, CERN, Geneva (1977).

*30.* MATLAB, Version 5.2; The Mathworks Inc., Natick, MA (1998).

*31.* M. Helmle, Y. K. Lee, P. J. E. Verdegem, X. Feng, T. Karlsson, J. Lugtenburg, H. J. M. de Groot, and M. H. Levitt, Anomalous rotational resonance spectra in magic-angle spinning NMR, *J. Magn. Reson.* **140,** (1999), in press.

*32.* D. Igner and D. Fiat, Single-crystal study of $^{13}C$ chemical shielding tensors in dimethyl maleic anhydride and acrylamide, *J. Magn. Reson.* **46,** 233–246 (1982).

*33.* J. Tegenfeldt, H. Feucht, G. Ruschitzka, and U. Haeberlen, $^{1}H$ and $^{13}C$ nuclear magnetic shielding tensors in solid pyromellitic acid dihydrate and malonic acid, *J. Magn. Reson.* **39,** 509–520 (1980).

*34.* K. Takegoshi, A. Naito, and C. A. McDowell, Intermolecular hydrogen-bonding effects on the $^{13}C$ NMR shielding tensor of the carbonyl carbon nucleus in a single crystal of dimedone, *J. Magn. Reson.* **65,** 34–42 (1985).

*35.* K. Takegoshi and C. A. McDowell, $^{13}C$ chemical shielding tensors in single crystals of tetraacetylethane, *Chem. Phys. Lett.* **123,** 159–163 (1986).

*36.* K. Takegoshi and C. A. McDowell, $^{13}C$ NMR studies of chemical-shielding tensors and molecular motion in meldrum's acid in the solid state, *J. Am. Chem. Soc.* **108,** 6852–6857 (1986).